Available online at www.sciencedirect.com
ScienceDirect
Trans. Nonferrous Met. Soc. China 25(2015) 2352−2360
Transactions of Nonferrous Metals Society of China
www.tnmsc.cn

Forming mechanism of ultrasonic vibration assisted compression

Xin-cun ZHUANG, Jia-peng WANG, Huan ZHENG, Zhen ZHAO

Institute of Forming Technology and Equipment, School of Materials Science and Engineering, Shanghai Jiao Tong University, Shanghai 200030, China

Received 28 October 2014; accepted 27 March 2015

Abstract: To study the mechanism of ultrasonic vibration assisted forming, the static and vibration assisted compression tests of aluminum 1050 were carried out via a 25 kHz high-frequency ultrasonic vibration device. It is found that vibration reduces the flow resistance and improves the surface topography. The force reduction level is proportional to the ultrasonic vibration amplitude. By using numerical simulation of static and vibration assisted compression tests, the deformation characteristics of material were investigated. Throughout the vibration, the friction between the materials and tools reduces. The stress superposition and friction effects are found to be two major reasons for reducing the force. However, the force reduction because of stress superposition and friction effects is still less than the actual force reduction from the tests, which suggests that softening effect may be one of the other reasons to reduce the force.

Key words: ultrasonic vibration; compression; stress superposition; friction effect

1 Introduction

Nowadays ultrasonic vibration has been widely used in metallurgy, welding, machinery, food processing and chemical industry. Lots of researches on ultrasonic vibration assisted forming showed that the forming force and the deformation resistance can be effectively reduced, and the formability as well as the surface quality can be improved by applying ultrasonic vibration. The effects derived from ultrasonic vibration assisted forming includes stress superposition [1], softening effect [2], hardening effect [3], the change in coefficient of friction [4] and friction vector effect [5]. To clarify the influences and even get more detail in the forming mechanism of the ultrasonic vibration assisted forming, three kinds of research strategies are generally adopted.

Experimental observation is one of the direct ways to investigate various phenomena related to the ultrasonic vibration, by designing the testing devices combined with ultrasonic vibration and analyzing the influence of various parameters on the forming quality and forming limit. HUNG and HUNG [6] established an ultrasonic vibration assisted hot upsetting system with a cooling mechanism to demonstrate the behavior of aluminum alloy under this condition. They found that axial ultrasonic vibration can reduce the forming force in hot upsetting, and the reduction magnitude decreased with the increase of temperature. However, there was less influence by the strain rate. JIMMA et al [7] applied radial ultrasonic vibration to the blank-holder and die as well during the deep drawing process. The experimental results showed that the limited deep drawing ratio can be increased by changing the frequency of vibration. In addition, the flange wrinkle disappeared when the amplitude increased.

The secondary strategy is the hybrid method by combining the experiment with the corresponding simulation work to investigate the unclear mechanism related to the ultrasonic vibration. The playback of some phenomena appeared in the experiments can be performed with the help of numerical simulation. Besides, the effect of various process parameters on the forming quality can be easily carried out based on the established numerical model, and more or less the parameters optimization can be realized. LIU et al [8] conducted the experiments of the cone tip upsetting with ultrasonic vibration and created the corresponding model

Foundation item: Project (51105250) supported by the National Natural Science Foundation of China; Project (P2015-13) supported by the State Key Laboratory of Materials Processing and Die & Mould Technology, Huazhong University of Science and Technology, China
Corresponding author: Zhen ZHAO; Tel: +86-21-62813430; E-mail: zzhao@sjtu.edu.cn
DOI: 10.1016/S1003-6326(15)63850-X

in ABAQUS. Based on the 2D axisymmetric model, stress and strain distributions and the effect of ultrasonic vibration on forming process can be easily observed. HAYASHI et al [9] built a numerical model of ultrasonic-vibration deep drawing in ABAQUS to analyze the drawing force and the distribution of stress and strain. The model can closely conform to the experiment results and quantitatively illustrate the mechanism how ultrasonic vibration improves the deep drawing characteristics.

Apart from the numerical method, some researchers turned to the theoretical models to uncover the mechanism of ultrasonic vibration. Till now, stress superposition effect and softening effect were studied. Against the stress superposition effect, CAI et al [10] deduced the constitutive equation under low-frequency vibration by a visco-elasticity plasticity model and described the strain and stress variability between the visco-elasticity and visco-plasticity. They found that both the yield strength and stress significantly reduced. YAO et al [11] built the acoustic softening model based on thermal activation theory and provided the relationship between the acoustic energy density and stress ratio. Once energy was large enough, it would facilitate the displacement between the crystals and reduce the dislocation density, which led to crystal dislocations associated with softening effect.

In this study, the hybrid strategy was adopted aiming at the discovery of the mechanism of ultrasonic vibration assisted forming process. Normally in a certain kind of plastic forming process like deep drawing there might be one or more effects occur simultaneously, thus tensile test or compression test was adopted here to explore the nature of each effect. An ultrasonic vibration system with frequency of 25 kHz was designed, with which the compression tests were conducted on a material testing machine. Then by combining the finite element simulation and experimental results, the influence of different effects was analyzed. The stress distributions of compression specimens were also discussed to explain the influence of ultrasonic vibration on the material mechanical property. In addition, stress superposition and friction effects were discussed in the analysis of the reasons for reducing the forming force.

2 Experimental

2.1 Testing device and plan

The typical ultrasonic vibration system is composed of ultrasonic generator, ultrasonic transducer, horn and tool, as shown in Fig. 1. Ultrasonic waves produced by the ultrasonic generator with nominal parameters 220 V/50 Hz/8A were transmitted periodicity along these parts in axial and radial directions. The maximum power of the system was 1500 W with resonant frequency of 25 kHz. The ultrasonic vibration device was mounted on a MTS−810 material testing machine. The specimen was placed on the top surface of the lower platen (i.e., tool). The compression speed was set as 1mm/min according to the conclusion of Ref. [12]. During the tests, the displacement and the force signals were measured simultaneously. The material used in the tests was soft aluminum 1050. The specimens were machined from the plate having thickness of 10 mm along the rolling direction into a shape of cylinder with diameter of 5 mm and height of 5 mm.

The ultrasonic vibration was applied to the lower platen directly contacted with the sample. In terms of the applied vibration duration, the experimental work can be classified into intermittent vibration assisted compression and full vibration assisted compression. In the full vibration assisted compression test, the start of the compression procedure with high-frequency vibration will result in sample slip, therefore, initial force was required to hold the sample. In the compression tests, the vibration was applied till the force was up to 100 N and persisted until the end of the compression.

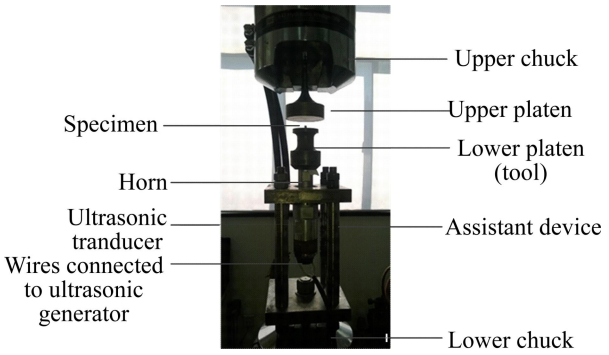

Fig. 1 Schematic of ultrasonic vibration assisted compression test

In order to compare the influence of ultrasonic vibration, conventional static compression and vibration assisted compression tests were performed, as per the testing plan shown in Table 1. P1 and P2 are conventional static compressions, and the amounts of ram displacement are 0.4 mm and 1.5 mm, respectively. A1 and A2 are full vibration assisted compression tests with the ram displacement of 0.4 mm. The vibration frequency is 25 kHz and the vibration amplitudes are 2 μm and 3 μm, respectively. U1, U2, U3 and U4 are the intermittent vibration assisted compression tests. The ram displacement is set as 1.5 mm.

Table 1 Testing plan

Case No.	Vibration period/mm	Ram displacement/mm	Frequency/ kHz	Amplitude/ μm
P1	−	0.4	−	−
P2	−	1.5	−	−
A1	0−0.4	0.4	25	2
A2	0−0.4	0.4	25	3
U1	0.3−0.5	1.5	25	2
U2	0.3−0.5	1.5	25	3
U3	0.3−0.7	1.5	25	2
U4	0.2−0.4	1.5	25	2

2.2 Force−displacement curve measurement

Since the specimen size is small, the machine compliance [13] will affect the accuracy of the final force−displacement curve. In order to eliminate the influence, the force−displacement curve of static compression test without specimen was measured firstly. As shown in Fig. 2, the force−displacement curve clearly shows two segments. During the first segment, the force increases slowly with inreasing the displacement in a short period. Thereafter, the force increases elastically with increasing the displacement in the secondary segment. The measured force−displacement curve of specimen shown in Fig. 2 is denoted as dotted line. By performing curve subtraction with regard to the force coordinate, the corrected force−displacement curve (dot dash line) could be obtained.

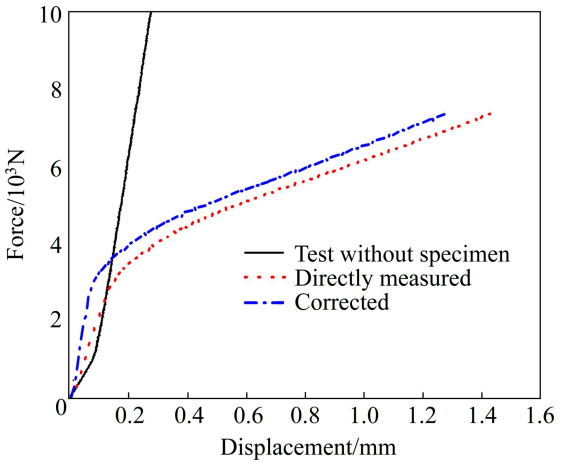

Fig. 2 Corrected force−displacement curve of compression test

3 Modeling of compression with and without vibration

The numerical simulations of compression tests were carried out using a commercial finite element code, ABAQUS/standard. Only half of the specimen was meshed using axisymmetric four-node elements, taking advantage of the symmetry. The upper and lower platens were assumed to be rigid bodies, modeled with analytical rigid. The un-deformed mesh profile is shown in Fig. 3. The material properties were derived from the conventional static compression tests. The engineering stress−strain curve was calculated assuming the deformation was homogeneous. And then the true stress−strain curve was converted from the engineering stress−strain curve to be applied in the simulation.

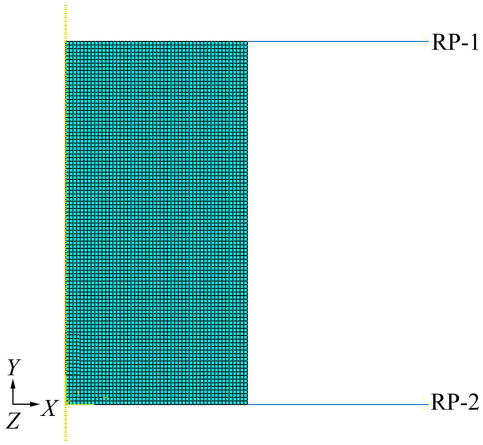

Fig. 3 Model of compression test (RP-1 and RP-2 denote the reference points of upper platen and lower platen, respectively)

Similar to the tests, ultrasonic vibration was applied to the lower platen in the numerical model with the same frequency of 25 kHz, by generating a sine wave displacement with the help of periodic type amplitude keyword. Taking U1 (the frequency of 25 kHz and the amplitude of 2 μm) as an example, detailed parameters are shown in Table 2. Wherein the cycle frequency is represented in the form of angular velocity, the start time is −0.00001 s representing quarter-cycle earlier. The initial amplitude is 0.001 mm, and the vibration is expressed in the form of sine wave, thus cosine parameter A=0 and sinusoidal parameter B=−0.001. The negative sign indicates the direction. Following this design, the displacement−time curve of the lower platen is shown in Fig. 4.

Table 2 Parameters of amplitude

Circular frequency/(rad·s^{-1})	Start time/s	Initial amplitude/mm	A	B
157028	−0.00001	0.001	0	−0.001

The simulation is divided into three steps, namely initial step, vibration step and final step, of which the detailed parameters can be found in Table 3. To save the actual computation time and meanwhile to well capture the vibration effect, the step time of vibration analysis step is set as 0.0012 s, which equals to 30 cycles of ultrasonic vibration.

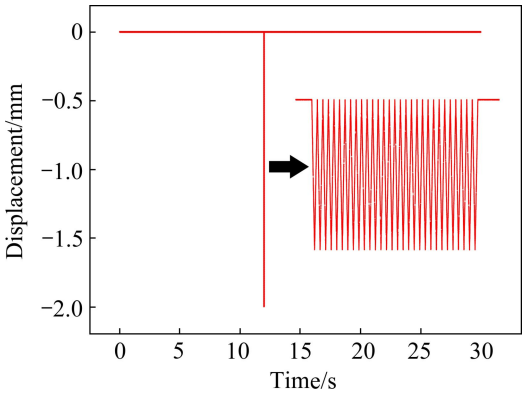

Fig. 4 Displacement−time curve of lower platen

Table 3 Analysis of step of vibration assisted compression simulation (Case U4)

Name	Time/s	Amplitude	
		Upper platen/mm	Lower platen
Initial step	12	−0.2	Fixed
Vibration step	0.0012	−0.00002	Periodic (25 kHz/2 μm)
Final step	17.9988	−0.29998	Fixed

4 Results and discussion

4.1 Force−displacement curves with ultrasonic vibration

Figure 5 shows the corrected force−displacement curve of case U1. The vibration was only applied to the lower platen during the period of the ram displacement from 0.3 mm to 0.5 mm. The total ram displacement after the upper platen contacting the specimen is 1.5 mm. According to the measured force−displacement curve, the vibration occurs at the plasticity stage, i.e., after yielding. It is clear that the force drops quickly, and then continues to rise along the previous trends. Once the vibration stops, the material loads again following the elastic path, and finally restores to the original plastic deformation region.

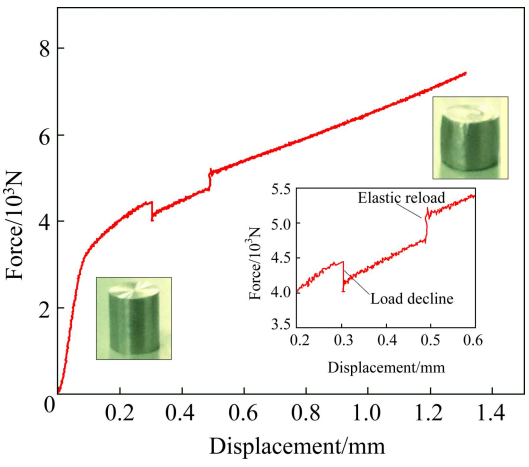

Fig. 5 Force−displacement curve of Case U1

The force−displacement curves of Cases P2, U1, U2 and U3 are plotted in Fig. 6, showing difference in the vibration step. Comparing the results of Cases U3 and U1, the force reductions are almost the same at the identical vibration period, and out of the vibration step, the curves show no difference. The reduction of Case U2 is significantly larger than that of Case U1, indicating that the force reduction is proportional to the vibration amplitude. Among these curves, the elastic reload could be clearly observed.

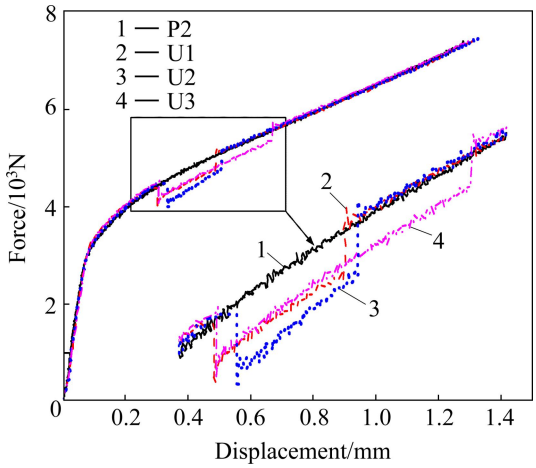

Fig. 6 Force−displacement curves of Cases P2, U1, U2 and U3

It is important to choose accurate friction coefficient between the platen and the sample during the simulation of vibration assisted compression test. By comparing the force−displacement curves obtained from experiment and the corresponding simulation, the friction coefficient of the static compression test could be determined. As shown in Fig. 7, Exp. is the results of Case P2, Simus. 1 to 4 represent the results of simulations with friction coefficients of 0, 0.1, 0.2 and 0.25, respectively. The ram displacement is 0.8 mm. The force of Simu. 1 is significantly lower than that of the test, particularly when the displacement reaches the large value. As to the friction coefficients of 0.20 and 0.25, with increasing the displacement, the force is slightly greater than that of the test, and the deviation is much greater with the increase of friction coefficient. Simu. 2 preferably coincides with the experimental result. Therefore, the friction coefficient of static compression test between upper and lower platen is assumed as 0.1.

As shown in Fig. 8, Exp. represents the force−displacement curve of Case U4, Simu. is the simulated one. The vibration force is under the condition of cyclical shocks. The average force during vibration is about

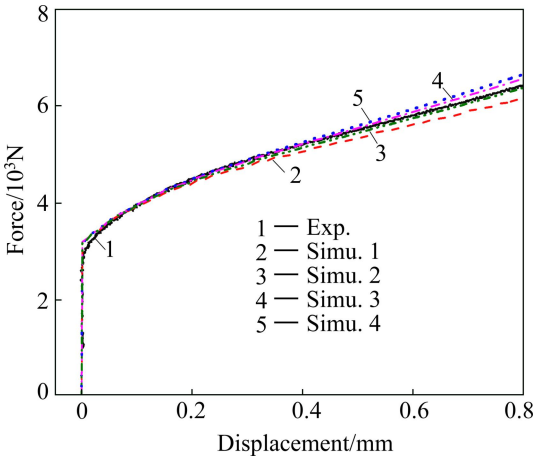

Fig. 7 Force−displacement curves of static compression test (Case P2)

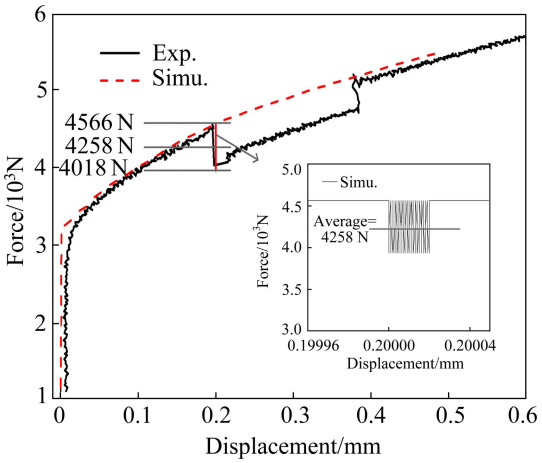

Fig. 8 Experimental and numerical results of vibration assisted compression test (Case U4)

4258 N, which is lower than 4566 N before applying the vibration. According to the guidance of MTS−810 material testing machine, the measured force during the vibration period is an averaged one. Thus, the average force from the simulation is higher than the measured one. Since only stress superposition could be reflect from the simulation, it is suggested that stress superposition is only one of the factors causing the vibration force reduction.

4.2 Stress and strain evolution

In the initial step, the stress contours of last four time steps are shown in Fig. 9. The maximum stress occurs at the outside of the sample in contact with the lower platen. The maximum stresses are 223.9, 224.1, 224.2 and 224.3 MPa, respectively, which gradually increase. The PEEQs (equivalent plastic strains) in these four time steps of the analysis are 0.0583, 0.0563, 0.0567 and 0.0571, respectively.

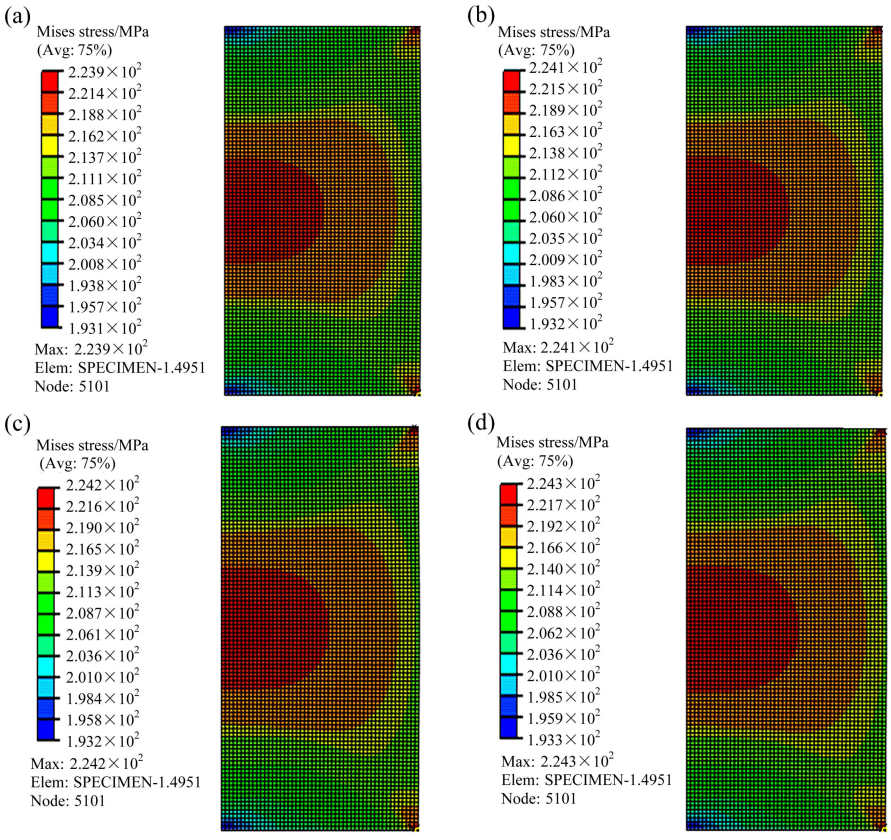

Fig. 9 Stress contours at last four time steps of initial step in vibration assisted compression simulation: (a) Step 1; (b) Step 2; (c) Step 3; (d) Step 4

The stress contours of the first six time steps of vibration step are shown in Fig. 10. The first time step is the final time step of the initial stage, and the maximum stress is 224.3 MPa. For the secondary time step, with the downward movement of lower platen, the stress distribution is changed, the maximum stress decreases to 206.3 MPa. During the third time step, the lower platen continues to move, further decline in the overall stress of material is found, and the maximum stress decreases to 190.2 MPa. In the fourth time step, the lower platen raises again. The maximum stress rises to 206.3 MPa. For the fifth time step, the lower platen rises to the initial position, the maximum stress recovers to 224.3 MPa and the stress distribution is similar to the initial state. So far a vibration cycle is finished.

At the final step of compression analysis, the stress contours of initial four time steps are shown in Fig. 11. The maximum stress is located between the lower platen and specimen border, and gradually increases from 224.3, 224.5 and 224.6 to 224.7 MPa.

4.3 Friction condition estimation

In Fig. 12, the overall trend of the force−displacement curve of Case A1 is consistent with that of static compression test, but the force is significantly lower during the elastic stage as well as the plastic stage until the end of the compression process. On the yield point, the corresponding force of P1 is 3090 N, while that of A1 drops to 2752 N. As to Case A2, the frequency of the vibration remains the same, while the vibration amplitude increases. The overall trend of the force−displacement curve of Case A2 is substantially similar to

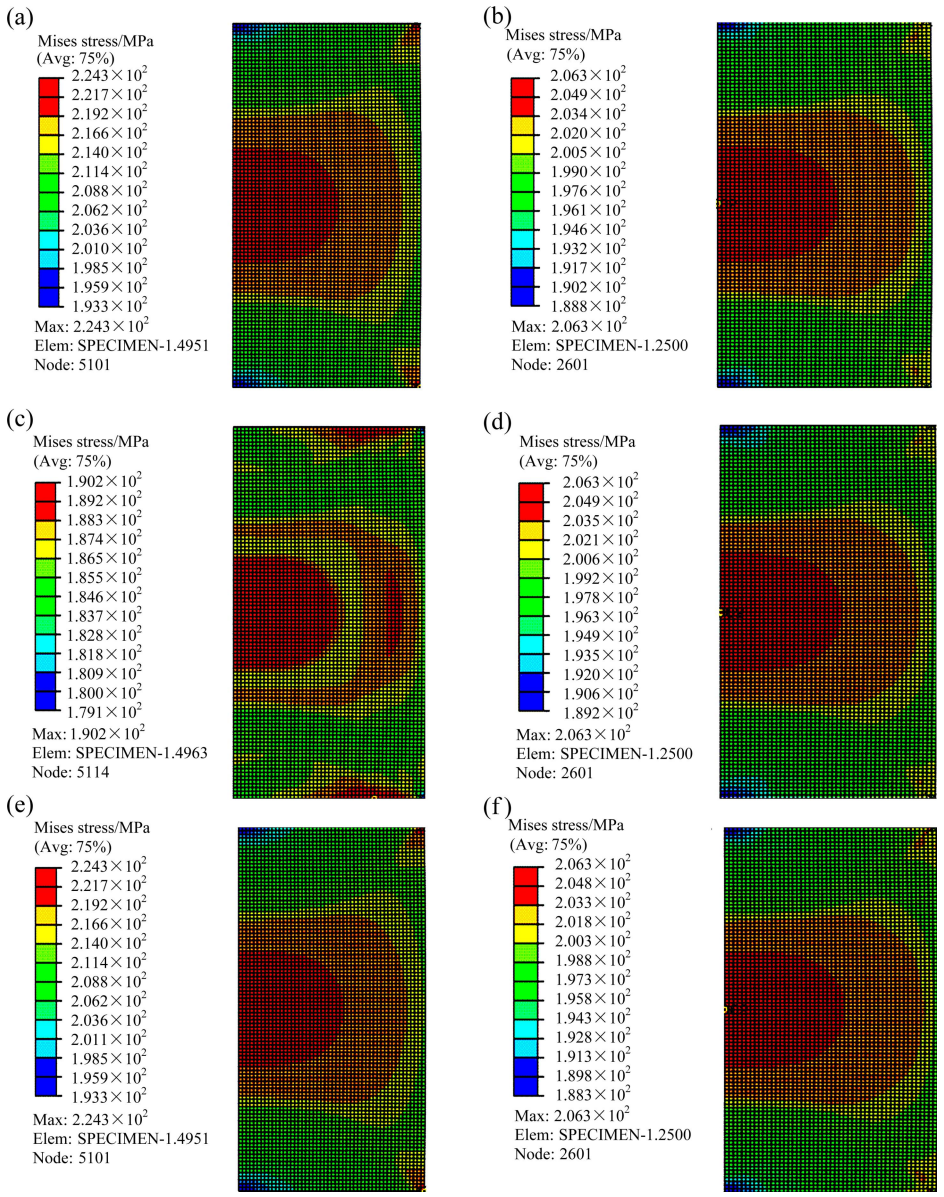

Fig. 10 Stress contours at first six time steps of vibration step in vibration assisted compression simulation: (a) Step 1; (b) Step 2; (c) Step 3; (d) Step 4;(e) Step 5; (f) Step 6

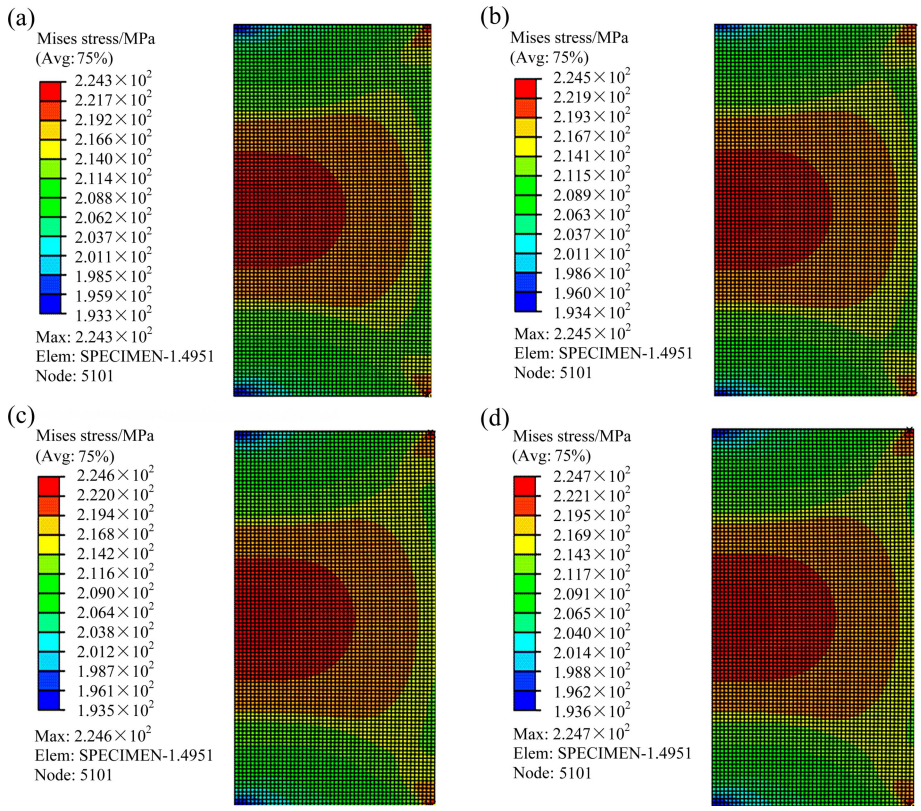

Fig. 11 Stress contours at first four time steps of final step in vibration assisted compression simulation: (a) Step 1; (b) Step 2; (c) Step 3; (d) Step 4

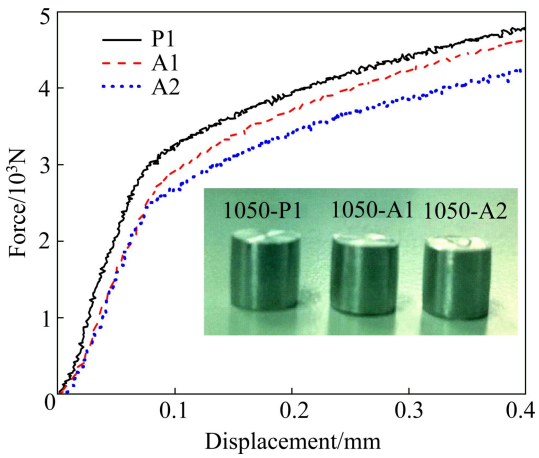

Fig. 12 Force−displacement curves of with and without full vibration

those of Cases P1 and A1. Compared Case A2 with Case A1, the elastic stage is similar, but in the plastic stage, the force suffers a further decline. It is suggested that the force reduction is because of the vibration, and the reduction level increases with increasing the vibration amplitude.

Scanning electron microscopy (SEM) was used to observe the effect of the vibration on the surface morphology of the compression test specimen, as shown in Fig. 13. The surface scratches of the specimen under

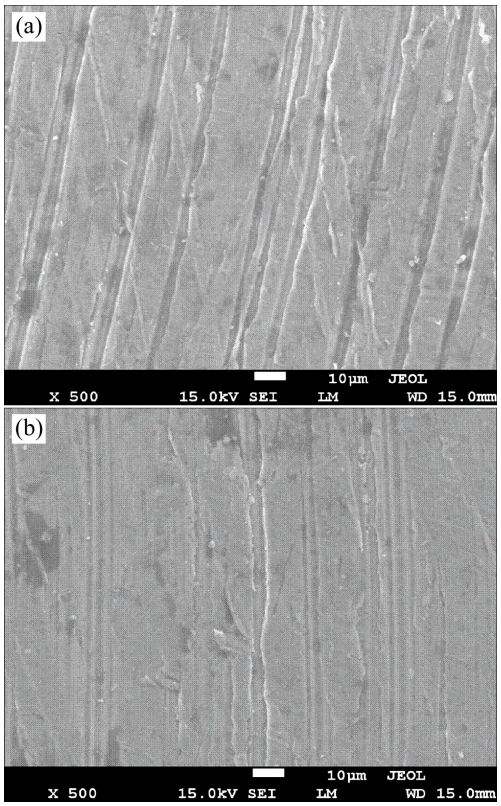

Fig. 13 Surface morphologies of compression test specimens: (a) P1; (b) A1

the vibration condition are smaller and less than those of static compression test, which suggests that the surface condition can be somewhat improved by applying the ultrasonic vibration.

Unlike the intermittent vibrations, it is difficult for the full vibration assisted compression to perform the corresponding simulation. One possible solution is to use an equivalent static compression test simulation. In the compression process, the friction condition may change with the reduction in height. The surface morphology changes during the compression, and therefore the friction coefficient also changes. However, it is hard to model the friction coefficient as a time-varying function, a constant value has been used in the numerical simulation. This constant friction coefficient can be considered as an average value of the time-varying friction during the forming processes.

The final part geometry changes with different friction coefficients. Due to the friction force at the die–specimen interface, the material in contact with the die is restricted to flow during the compression process. Hence, the cylindrical sample is deformed into a "barrel" shape, which is known as the "barreling" phenomenon. Therefore, the amount of barreling is a good measure of the magnitude of the friction involved during the compression operation. To quantify the geometry change caused by the barreling, two area ratios of K_t and K_b, are defined as the ratio of top surface area (S_t) to maximum section area (S_m) and the ratio of bottom surface area (S_b) to maximum section area, respectively. Initially, with the same friction coefficient at the upper die−specimen interface and the lower die− specimen interface, the values of K_t and K_b are supposed to be equal. Thus, it is possible to establish the relationship between the area ratio and the friction coefficient by performing a series of simulations with different friction coefficients. The simulations were stopped at the same final sample height of 1.2 mm, and then the area ratios were calculated. The relation between the area ratio and the friction coefficient is shown in Fig. 14. As expected, once the friction coefficient increases, more significant barreling is observed and the area ratio decreases.

The dimensions of compression specimens are shown in Table 4. P2 is a conventional static compression test specimen, and its area ratio is around 0.9590. According to the plot in Fig. 14, the friction coefficient is close to 0.1. Compared with the simulation results shown in Fig. 7, the choice of friction coefficient of 0.1 is consistent. A1 is the full vibration compression. For Case A1, the diameter of bottom surface (D_b) is greater than that of top surface (D_t). D_m denotes the diameter of the maximum section area. K_t is similar with the conventional static compression, while K_b is greater than K_t. The corresponding friction coefficient at the

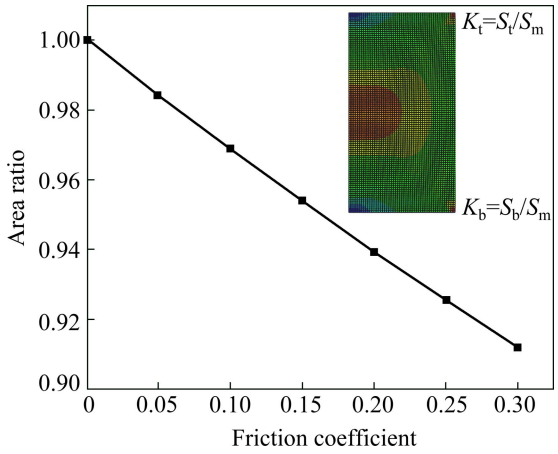

Fig. 14 Relationship between friction coefficient and area ratio

Table 4 Dimensions of compression specimens

Case No.	D_b/mm	D_t/mm	D_m/mm	K_t	K_b
P2	5.210	5.200	5.310	0.9627	0.9590
A1	5.270	5.230	5.320	0.9665	0.9813

lower platen−specimen interface is about 0.06. This is suggested that the vibration throughout the compression process can reduce the friction between the sample and the lower platen.

Further studies are about the impact of the changes of friction conditions on the force reduction. In intermittent vibration step, the friction coefficient is 0.1 between the specimen and the lower platen. According to the full vibration assisted compression simulation results, the equivalent friction coefficient of full vibration process is 0.06. So, the coefficient of friction is set as 0.06, and the other simulation parameters remain unchanged. The force−displacement curve derived from the simulation is shown in Fig. 15. The average force of the vibration phase reduces from 4258 N to 4214 N, which is much closer to the actual test results. This is

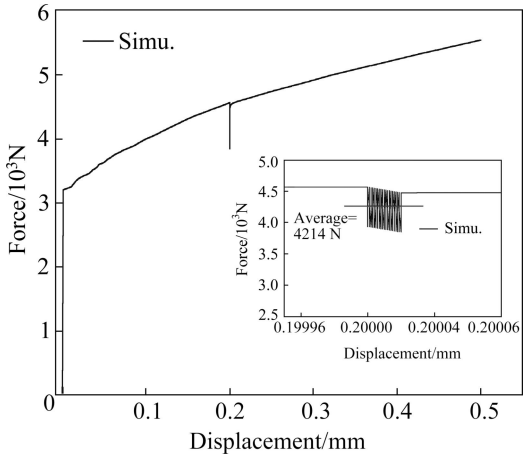

Fig. 15 Force−displacement curve of intermittent vibration assisted compression simulation

suggested that the intermittent vibration step is affected by the friction condition. However, the stress superposition and friction effects cannot fully lead to a large force reduction. According to the results of full vibration assisted compression test, softening effect may be one of the other reasons to reduce the force.

5 Conclusions

1) In the full vibration assisted compression test, the force reduces apparently. The reduction level is proportional to the amplitude of ultrasonic vibration. And the vibration contributes to improve the surface morphology.

2) In the intermittent vibration assisted compression test, significant force reduction occurs, and then the force continues to rise along the previous trends. Once the vibration stops, the material loads again after short elastic reload and finally restores to the original plastic deformation region.

3) During the vibration step, the stress changes periodically. The force reduction because of stress superposition and friction effects is still less than the actual force reduction from the tests, thus softening effect may be one of the other reasons to reduce the force.

References

[1] EAVES A E, SMITH A W, WATERHOUSE W J, SANSOME D H. Review of the application of ultrasonic vibrations to deforming metals [J]. Ultrasonics, 1975, 13(4): 162−170.

[2] KIRCHNER H O K, KROMP W K, PRINZ F B, TRIMMEL P. Plastic deformation under simultaneous cyclic and unidirectional loading at low and ultrasonic frequencies [J]. Materials Science and Engineering A, 1985, 68(2): 197−206.

[3] DAUD Y, LUCAS M, HUANG Z H. Modelling the effects of superimposed ultrasonic vibrations on tension and compression tests of aluminium [J]. Journal of Materials Processing Technology, 2007, 186(1): 179−190.

[4] LEE K H, LEE S K, KIM B M. Advanced simulation of die wear caused by wire vibrations during wire-drawing process [J]. Transactions of Nonferrous Metals Society of China, 2012, 22(7): 1723−1731.

[5] NGAILE G, BUNGET C. Influence of ultrasonic vibration on microforming [J]. Transactions of NAMRI/SME, 2008, 36: 137−144.

[6] HUNG Jung-chung, HUNG Ching-hua. The influence of ultrasonic-vibration on hot upsetting of aluminum alloy [J]. Ultrasonics, 2005, 43(8): 692−698.

[7] JIMMA T, KASUGA Y, IWAKI N, MIYAZAWA O, MORI E, ITO K, HATANO H. An application of ultrasonic vibration to the deep drawing process [J]. Journal of Materials Processing Technology, 1998, 80: 406−412.

[8] LIU Y X, SUSLOV S, HAN Q Y, XU C, HUA L. Microstructure of the pure copper produced by upsetting with ultrasonic vibration [J]. Materials Letters, 2012, 67(1): 52−55.

[9] HAYASHI M, JIN M, THIPPRAKMAS S, MURAKAWA M, HUNG Jung-chung, TSAI Yu-chung, HUNG Ching-hua. Simulation of ultrasonic-vibration drawing using the finite element method (FEM) [J]. Journal of Materials Processing Technology, 2003, 140(1): 30−35.

[10] CAI Gai-ping, LIU Zhen, ZHANG Hui. Volume effect analyses of metal deformation with low-frequency pulse vibration [J]. Forging & Stamping Technology, 2008, 33(5): 155−159.

[11] YAO Z H, KIM G Y, WANG Z H, FAIDLEY L, ZOU Q Z, MEI De-qing, CHEN Zi-chen. Acoustic softening and residual hardening in aluminum: Modeling and experiments [J]. International Journal of Plasticity, 2012, 39: 75−87.

[12] HUANG Z H, LUCAS M, ADAMS M J. Study of ultrasonic upsetting under radial and longitudinal die vibration [J]. Materials Science Forum. 2003, 440: 389−396.

[13] KALIDINDI S R, ABUSAFIEH A, EL-DANAF E. Accurate characterization of machine compliance for simple compression testing [J]. Experimental Mechanics, 1996, 37(2): 210−215.

超声振动辅助压缩成形机理

庄新村，王家鹏，郑 欢，赵 震

上海交通大学 材料科学与工程学院，塑性成形技术与装备研究院，上海 200030

摘 要：为研究超声振动辅助成形的内在机理，设计一套 25 kHz 高频超声振动装置，配合试验机进行 1050 铝合金静态及振动辅助条件下的压缩试验。实验发现，振动有利于降低材料的流动抗力，同时有助于改善试样表面形貌；成形力的降幅与所施加超声振动的振幅成比例关系。结合有限元数值模拟，研究材料在超声振动辅助压缩条件下的变形特点，发现在振动阶段，试样与模具接触面之间的摩擦条件得以改善。此外，应力叠加和摩擦条件改善是振动阶段成形力降低的两个原因，但两者的降幅总和小于实验中测得的降幅，因此软化效应是成形力降低的另一原因。

关键词：超声振动；压缩；应力叠加；摩擦效应

(Edited by Mu-lan QIN)